

Metadata of the chapter that will be visualized in SpringerLink

Book Title	Nano and Biotech Based Materials for Energy Building Efficiency	
Series Title		
Chapter Title	Nanocellulose Aerogels as Thermal Insulation Materials	
Copyright Year	2016	
Copyright HolderName	Springer International Publishing Switzerland	
Corresponding Author	Family Name	Duong
	Particle	
	Given Name	Hai M.
	Prefix	
	Suffix	
	Division	Department of Mechanical Engineering
	Organization	National University of Singapore
	Address	Singapore, 117575, Singapore
	Email	mpedhm@nus.edu.sg
Author	Family Name	Nguyen
	Particle	
	Given Name	Son T.
	Prefix	
	Suffix	
	Division	Department of Mechanical Engineering
	Organization	National University of Singapore
	Address	Singapore, 117575, Singapore
	Email	
Abstract	<p>There is a high demand of energy consumption due to the increasing population, industrial expansion, and development plans. However, the increasing cost of energy and the negative impact on the environment by energy production plants have resulted in the need to find means to substantially reduce energy consumption. Buildings are one of the main factors contributing to the world energy consumption. About two-thirds of the total energy is used for buildings. It is essential to reduce energy consumption of buildings by finding more effective thermal insulation materials. Cellulose is a green, cheap, and abundant material with low thermal conductivity. Its combination with aerogel structure forms a novel and effective heat insulation material known as cellulose aerogel. Cellulose aerogels can be fabricated from bacterial cellulose, wood/paper pulps, or cellulosic wastes. The aerogels become water-repellent after being treated with silane reagents via a chemical vapor deposition (CVD) method. They show highly porous structures with good flexibility, high stability, and extremely low thermal conductivities. These characteristics make them promising for thermal insulation applications.</p>	



Chapter 15

Nanocellulose Aerogels as Thermal Insulation Materials

Hai M. Duong and Son T. Nguyen

Abstract There is a high demand of energy consumption due to the increasing population, industrial expansion, and development plans. However, the increasing cost of energy and the negative impact on the environment by energy production plants have resulted in the need to find means to substantially reduce energy consumption. Buildings are one of the main factors contributing to the world energy consumption. About two-thirds of the total energy is used for buildings. It is essential to reduce energy consumption of buildings by finding more effective thermal insulation materials. Cellulose is a green, cheap, and abundant material with low thermal conductivity. Its combination with aerogel structure forms a novel and effective heat insulation material known as cellulose aerogel. Cellulose aerogels can be fabricated from bacterial cellulose, wood/paper pulps, or cellulosic wastes. The aerogels become water-repellent after being treated with silane reagents via a chemical vapor deposition (CVD) method. They show highly porous structures with good flexibility, high stability, and extremely low thermal conductivities. These characteristics make them promising for thermal insulation applications.

15.1 Introduction

Cellulose is one of the most common and abundant polymers on the planet. It is widely used in industry and normal life. Cellulose is a non-branched macromolecule containing ringed glucose molecules. Its repeat unit consists of two anhydroglucose rings linked together through oxygen covalently bonded to C1 of one glucose ring and C4 of the adjoining ring. This bond is known as the β 1–4 glucosidic bond. Intra- and interchain hydrogen bonding makes cellulose a relatively stable polymer (Cai et al. 2008; Cervin et al. 2012; Chang and Zhang 2011;

H.M. Duong (✉) · S.T. Nguyen
Department of Mechanical Engineering, National University of Singapore,
Singapore 117575, Singapore
e-mail: mpedhm@nus.edu.sg

29 Kalia et al. 2011; Wicklein et al. 2015; Pour et al. 2015). Van der Waals and
30 intermolecular hydrogen bonds promote parallel stacking of multiple cellulose
31 chains forming elementary fibrils. These fibrils then aggregate to form larger
32 microfibrils in the plant cell wall, which also aggregate into macroscopic fibers.
33 These microfibrils have typically a diameter of about 10–30 nm and are made up of
34 30–100 cellulose molecules in extended chain conformation and provide mechanical
35 strength to the fiber (Eichhorn et al. 2010; Mieck et al. 1994; Moon et al. 2011).

36 Cellulose fibers have many potential applications because of their advantages
37 such as abundantly available, low weight, biodegradable, cheaper, renewable, low
38 abrasive nature, and good mechanical properties. Cellulose fibers can be classified
39 according to their origin and grouped as follows: (1) leaf: abaca, pineapple, sisal,
40 banana, etc.; (2) seed: cotton; bast: flax, hemp, etc.; (3) fruit: coir, kapok, etc.;
41 (4) grass: bagasse, bamboo, etc.; and (5) stalk: straw (cereal) (Eichhorn et al. 2010;
42 Kalia et al. 2011; Klemm et al. 2011; Mieck et al. 1994; Moon et al. 2011; Oshima
43 et al. 2014). Commonly used plant fibers are cotton, jute, hemp, flax, ramie, sisal,
44 coir, henequen, and kapok. Properties of cellulose fibers are affected by many
45 factors such as variety, climate, harvest, maturity, retting degree, decortications,
46 disintegration (mechanical, steam explosion treatment), fiber modification, textile,
47 and technical processes (spinning and carding). Cellulose fibers with moduli up to
48 40 GPa can be separated from wood by chemical-pulping process. Such fibers can
49 be further subdivided into microfibrils with elastic modulus of 70 GPa.

50 Cellulose nanofibers (CNFs) have a high potential to be used in many different
51 areas such as reinforcement in development of nanocomposites. Many studies have
52 been done on isolation and characterization of CNFs from various sources.
53 Cellulose nanofibers can be extracted from the cell walls by simple mechanical
54 methods or by a combination of both chemical and mechanical methods (Eichhorn
55 et al. 2010; Kalia et al. 2011; Klemm et al. 2011; Mieck et al. 1994; Moon et al.
56 2011; Oshima et al. 2014). Cellulose nanofibers are extracted from the agricultural
57 residues, wheat straw, and soy hulls, by a chemomechanical technique. The wheat
58 straw nanofibers have diameters in the range of 10–80 nm and lengths of a few
59 thousand nanometers. By comparison, the soy hull nanofibers have diameters of
60 20–120 nm and shorter lengths than the wheat straw nanofibers. Zimmermann et al.
61 (2004) separated nanofibrillated cellulose at the greatest possible lengths and
62 diameters below 100 nm from different starting cellulose materials by mechanical
63 dispersion and high-pressure (up to 1500 bar) homogenization processes. The
64 treatment resulted in nanoscaled fibril networks.

65 Aerogels have been well known as highly porous solids that hold air within their
66 pores. As a result, their lightness, low heat conductivity, and large surface area
67 make them ideal for possible applications as heat insulators, particle filters, particle
68 trappers, and catalyst supports (Innerlohinger et al. 2006; Gesser and Goswami
69 1989; Bheekhun et al. 2013; Bryning et al. 2007; Pierre and Pajonk 2002; Nguyen
70 et al. 2012). The combination of aerogel structure and cellulose fibers forms cel-
71 lulose aerogel, a new kind of aerogel, which is green, cheap, and abundant.
72 Cellulose-based aerogels were developed during the 1950s by Stamm and
73 coworkers (1950). However, little further development occurred until the 2000s.

74 Most research efforts have been in aerogel processing and in some isolated cases the
75 subsequent functionalization of the aerogel via coatings. The environmentally
76 friendliness, low thermal conductivity (0.040–0.050 W/m K) of cellulose, and the
77 highly porous aerogel structure facilitate the heat insulation property of cellulose
78 aerogels and thus open a new chapter in thermal insulation (Baetens et al. 2011; Fan
79 et al. 2014; Al-Homoud 2005; Briga-Sá et al. 2013; Jelle 2011). The total global
80 aerogel market is forecast to grow at a very high rate of 19.3 % from 2012 to 2017
81 and reach global revenues of \$332.2 million by 2017 (Nguyen et al. 2014). In
82 particular, the thermal and acoustic insulation sector accounted for 82.3 % of all
83 revenues in 2012 and shows the most potential growth with a five-year compound
84 annual growth rate of 20.2 % from 2012 through 2017. Therefore, cellulose
85 aerogels will have a very bright future in the global insulation market.

86 15.2 Advanced Cellulose Aerogels for Heat Insulation 87 of Buildings

88 There have been several works on cellulose aerogels. Based on the cellulose source,
89 cellulose aerogels can be synthesized from bacterial cellulose, wood/paper pulp, or
90 wastes.

91 15.2.1 Cellulose Aerogels Prepared from Bacterial Cellulose

92 15.2.1.1 Fabrication Methods

93 Bacterial cellulose (BC) was first reported by Adrian Brown while working with
94 *Bacterium aceti* in 1886 (cite from ...). A solid mass is formed at the surface of
95 vinegar fermentation medium and is commonly used in homemade vinegar pro-
96 duction (Oshima et al. 2014; Cai et al. 2012; Sai et al. 2013, 2014; Pircher et al.
97 2014; Liebner et al. 2010). The constituent was later identified as cellulose, and the
98 name *Bacterium xylinum* was assigned to the microorganism responsible for its
99 synthesis. Since its discovery, several names were given to this bacterium including
100 *Acetobacterium xylinum* and *Bacterium xylinodes*. It was later named as *Acetobacter*
101 *xylinum* and became the official name according to the International Code of
102 Nomenclature of Bacteria (Cannon and Anderson 1991; Yamanaka et al. 1989).
103 Now, this Gram-negative, strictly aerobic bacteria are referred to as species
104 *Gluconacetobacter xylinus*. Although BC can be produced from the species of
105 genera *Achromobacter*, *Alcaligenes*, *Aerobacter*, *Agrobacterium*, *Azotobacter*,
106 *Gluconacetobacter*, *Pseudomonas*, *Rhizobium*, *Sarcina*, *Dickeya*, and *Rhodobacter*,
107 only species from genus *Gluconacetobacter* can produce cellulose at commercial
108 levels.

BC is produced by acetic acid bacteria in both synthetic and non-synthetic media through partial oxidation of ethanol. As mentioned above, *Acetobacter xylinum* is the most studied and the most efficient BC producer that manages to assimilate various sugar sources such as glucose, sucrose, and coconut milk and yields high level of cellulose in liquid media. It needs to be given the optimal conditions in terms of temperature, oxygen supply, and nutrients to be able to synthesize cellulose (Liebner et al. 2010; Liang et al. 2015; Keshk 2014; Sai et al. 2014; Pircher et al. 2014). As a nutrient source, several growth media exist, one that is very common is a mixture introduced by Schramm and Hestrin in 1954, which consists of 20 g l⁻¹ glucose, 5 g l⁻¹ peptone, 5 g l⁻¹ yeast extract, 1.15 g l⁻¹ citric acid monohydrate, and 6.8 g l⁻¹ Na₂HPO₄ 12 H₂O (Hestrin and Schramm 1954). Process is active at pH 3–7 and at temperature between 25 and 30 °C. It was reported that almost 30 % of bacterial fermentation cost belongs to the cost of fermentation medium. High cost and low-yield production have limited the industrial production of BC and its commercial application (Liebner et al. 2010; Liang et al. 2015; Keshk 2014; Sai et al. 2014; Pircher et al. 2014). Therefore, it is important to look for a new cost-effective carbon source with shorter fermentation process for high-yield BC production. The BC hydrogel then undergoes a drying process to be converted to BC aerogel. To maintain the porous structure of the BC hydrogel, two drying ways are usually used: freeze drying and supercritical point drying. In the first method, the hydrogel is frozen by liquid nitrogen or a refrigerator, and then, the ice in the sample is removed by sublimation directly with vacuum. In the supercritical drying method, the BC hydrogel is subject to thorough solvent exchange with ethanol to form BC alcogel. Then, ethanol is replaced by liquid CO₂. After that, CO₂ is converted into the supercritical state and slowly released to ambient pressure. Unlike plant cellulose, BC does not require extra processing to remove unwanted impurities and contaminants such as lignin, pectin, and hemicellulose, thus being able to retain a greater degree of polymerization.

15.2.1.2 Morphology

Scanning electron micrographs (SEM) of BC aerogels (Fig. 15.1) reveal a hierarchical order of the open-porous network, which consists of a well-developed macropore system formed from disorderly dispersive 20–80 nm cellulose fibers. Apart from macropores, Liebner et al. (2010) found that BC aerogels also have a mesoporous substructure (Liebner et al. 2010). Nitrogen sorption experiments show that the mesopores considerably contribute to the total pore volume as the obtained isotherms are of type IV. The mesopore diameter is about 10 nm, and the surface area and pore volume are about 160–200 m² g⁻¹ and 0.5 cm³ g⁻¹, respectively. BC aerogels possess very low densities of around 6.7–8.3 mg cm⁻³. Their porosity is about 99.6 %. X-ray diffraction (XRD) spectra of BC aerogels show three characteristic peaks centered at 14.78°, 16.98°, and 22.78°, corresponding to the typical (110), (110), and (020) planes of cellulose I, respectively.

Fig. 15.1 BC aerogel
(Pircher et al. 2014)

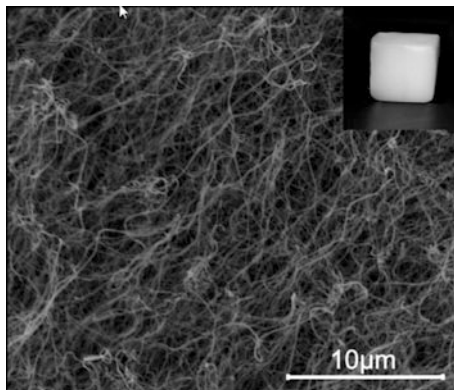
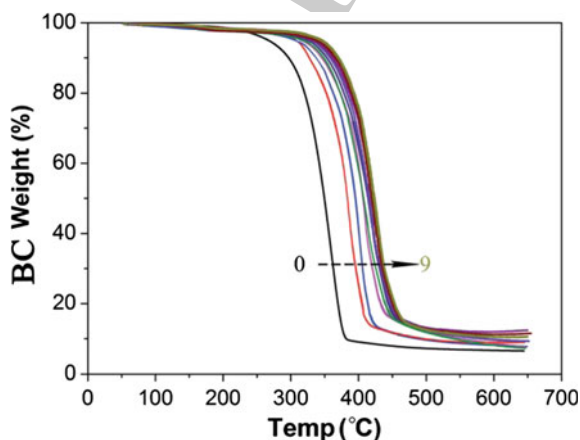


Fig. 15.2 TGA result of BC aerogels (Sai et al. 2014)



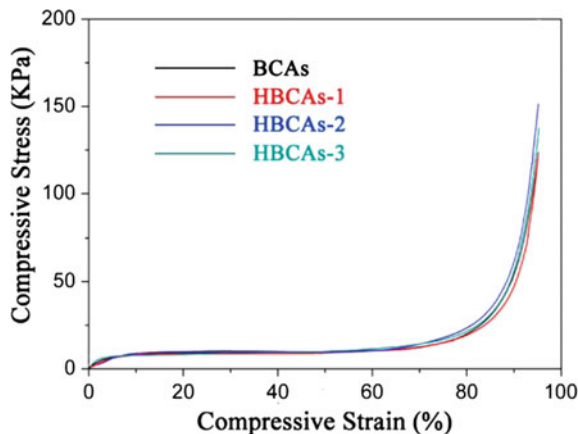
15.2.1.3 Thermal Properties

Thermogravimetric analysis (TGA) results (Fig. 15.2) show that BC aerogels start to decompose at 250 °C. They lose 5 % of their weight at 265 °C, 10 % of their weight at 290 °C, and completely degrade at about 380 °C. They exhibit an extremely low thermal conductivity of $0.0295 \text{ W m}^{-1} \text{ K}^{-1}$ (Sai et al. 2014), almost the same as that of silica aerogels, indicating that they are promising for thermal insulation applications.

15.2.1.4 Mechanical Properties

The BC aerogels have a 3D Web-like morphology formed from a large number of hydrogen bonds between the BC nanofibers. This makes them strong and flexible. Figure 15.3 shows compressive curves of BC aerogels. It was found that they

Fig. 15.3 Compressive curves of BC aerogels (Sai et al. 2015)



161 possess a compression modulus of 0.27 MPa in Sai et al.'s work (Sai et al. 2013).
 162 Pircher et al. (2014) found that BC aerogels have specific modulus values of 19–
 163 25 MPa cm³ g⁻¹, which are remarkably high compared to other porous materials.
 164 For example, for a polyurethane foam of a density of 90 mg cm⁻³, a specific
 165 modulus of 7.8 MPa cm³ g⁻¹ was previously reported. A lower specific modulus of
 166 about 4 cm³ g⁻¹ was reported for silica aerogel.

15.2.2 Cellulose Aerogels Prepared from Wood/Paper Pulp

15.2.2.1 Fabrication Methods

169 Cai et al. (2008) fabricated cellulose aerogels from filter paper pulp, Whatman
 170 cellulose powder, cotton linter pulp, and tunicate cellulose. The solvent mixtures
 171 NaOH/urea/H₂O (7:12:81 w/w) and LiOH/urea/H₂O (4.6:15:80.4 w/w) were pre-
 172 cooled to -12 °C. Then, the desired amount of the cellulose sample was imme-
 173 diately dispersed into the solvent system under vigorous stirring for 10 min at
 174 ambient temperature to obtain a transparent cellulose solution (0.5–7 wt%). The
 175 cellulose solution was subjected to centrifugation at 5000 rpm for 10 min at 5 °C to
 176 remove air bubbles. The resulting solution was cast on a glass plate to give a
 177 0.5-mm-thick layer and immersed into various coagulation baths for regeneration.
 178 The regeneration conditions were wt% H₂SO₄ aqueous solution at 0–60 °C for
 179 5 min, ethanol–H₂O with different volume ratios at 20 °C for 2 h, methanol at 20 °C
 180 for 2 h, acetone at 20 °C for 2 h, isopropanol at 20 °C for 2 h, and tert-butanol at
 181 20 °C for 2 h. The regenerated cellulose films were washed with excess deionized
 182 (DI) water to remove the residual chemical reagents. The cellulose hydrogels were
 183 then dried by supercritical drying or freeze-drying methods.

184 Wang et al. (2012) pretreated microcrystalline cellulose, filter paper pulp,
185 bleached sulfite pulp, cellulose I, and cellulose II (from beech wood holocellulose)
186 with ethylene diamine (EDA) for 24 h at room temperature, and filtered and
187 freeze-dried to get the cellulose-EDA complex. This complex was added into a 8 %
188 LiCl/dimethyl sulfoxide (DMSO) solution. The mixture was stirred at room tem-
189 perature for 24 h, followed by stirring at 75 °C for several hours to give clear
190 solution. The cellulose solution was poured into a glass dish to form 1-mm-thick
191 layer and immersed in ethanol for regeneration–gelation. The gel was thoroughly
192 washed by ethanol, then by water to remove LiCl, DMSO, and EDA. The hydrogel
193 was solvent-exchanged to ethanol and freeze-dried to form the final aerogel.

194 Instead of using NaOH/urea/H₂O, LiOH/urea/H₂O, or LiCl/DMSO solutions,
195 Liebner et al. dissolved cellulose in a melting N-methylmorpholine-N-oxide
196 (NMMO) and N-benzyl-morpholine-N-oxide (NBnMO) mixture (Liebner et al.
197 2007, 2008). The cellulose dope was poured into the desired form by molds and
198 cooled to room temperature. NMMO/cellulose moldings were regenerated by
199 adding ethanol or DMSO or mixtures of both in an end-over-end mixer for 24 h.
200 Then, the regeneration was repeated with another 10 ml of the corresponding
201 solvent for another 24 h. Supercritical drying was used to convert the gel to aerogel.

202 Cellulose can also be dissolved in hydrophilic ionic liquids, such as
203 1-allyl-3-methylimidazolium chloride (AMImCl). In Li et al.'s work (2011), wood
204 flour was mixed with AMImCl in a 500-mL beaker. The beaker was immersed in an
205 oil bath at 80 °C under constant stirring for 4 h to form a brownish homogeneous
206 mixture. The homogeneous viscous solution was transferred to appropriate molds
207 and sealed individually. All samples underwent cyclic freeze–thaw (FT) treatment.
208 The typical FT process is described as follows: The sample was frozen at –20 °C
209 for 10 h; then, it was vacuum-thawed for 6 h to room temperature. After undergoing
210 several FT cycles, all samples were immersed in the first coagulation bath with
211 deionized water. The bath was replenished at least three times until no Cl[–] was
212 detected using AgNO₃ solution. The samples were then dried using supercritical
213 drying with CO₂.

214 In Chen's group's research (Chen et al. 2011), wood fibers were dewaxed with a
215 mixture of benzene and ethanol. Then, the lignin in the sample was removed using
216 an acidified sodium chlorite solution at 75 °C for 1 h. Hemicellulose, residual
217 starch, and pectin were removed by KOH treatment. Highly purified cellulose fibers
218 were prepared by further treating the samples with a 1 wt% HCl solution at 80 °C
219 for 2 h and thoroughly washing them with distilled water. Finally, about 100 ml of a
220 solution containing purified cellulose fibers was placed in a common ultrasonic
221 generator with a frequency of 19.5–20.5 kHz and equipped with a cylindrical
222 titanium alloy probe tip 2.5 cm in diameter. The subsequent ultrasonication was
223 conducted for 30 min at an output power of 1200 W, resulting in the cellulose
224 hydrogels. The samples were then placed in a refrigerator at –18 °C for more than
225 24 h. Afterward, the samples were subjected to freeze-drying to allow frozen water
226 in the materials to sublime directly from the solid phase to the gas phase.

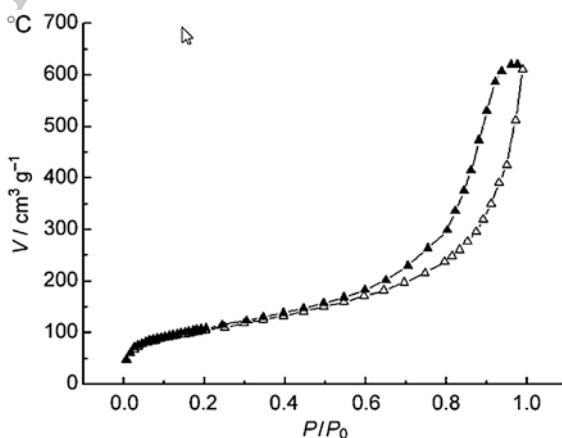
15.2.2.2 Morphology

Cai et al. found that the cellulose aerogels fabricated from NaOH/urea or LiOH/urea had porosities of 73.9–98.0 % with Brunauer–Emmett–Teller (BET) surface areas of 260–495 m²/g (Cai et al. 2008). For the NaOH/urea method, the porosity of the aerogels increased slightly from 85.5 to 88.7 % when increasing regeneration temperature (0–60 °C) in a regeneration bath of 5 wt% H₂SO₄. The LiOH/urea system exhibited a similar behavior. All the nitrogen adsorption/desorption isotherms obtained were of type IV (Fig. 15.4). BET surface area values of samples dried by water freeze-drying were smaller than those of samples dried with tert-butanol and CO₂. As shown in Fig. 15.5, the aerogels obtained by freeze-drying from water and tert-butanol showed differences in morphology between the surface and the inside (examined on cross sections). These aerogels had highly porous networks on the surface, consisting of fibrils less than 100 nm wide, but some parts of the sample obtained from water contained film-like structures spanning between the fibrils (Fig. 15.5b). These films could have resulted from the growth of relatively large ice crystals expelling fine fibrils of cellulose. This may be the cause of the small BET surface area value of the water freeze-dried material as compared with the other two samples. On the other hand, the inner parts of all the aerogel samples viewed on the cross sections displayed more uniform, nanometer-sized pore structures composed of fibrillar networks (Fig. 15.5d, h and l). The supercritical CO₂-dried material had a more homogenous structure, being the same on the surface and the cross section. These features confirm that supercritical CO₂ drying is the best method in preserving the liquid-swollen gel structure upon drying.

For the cellulose aerogels synthesized with the LiCl/DMSO system, the surface of the aerogels showed somewhat collapsed structure; in contrast, the inside observed on fractured cross sections showed cellulose networks of unique structure. The bulk of aerogel was composed of long and fairly straight fibrils interconnected with one another to form three-dimensional networks with large interstitial spaces (Wang et al. 2012). The difference between the surface and inside is likely to result

AQ2

Fig. 15.4 Nitrogen adsorption/desorption isotherm of the cellulose aerogels (Cai et al. 2008)



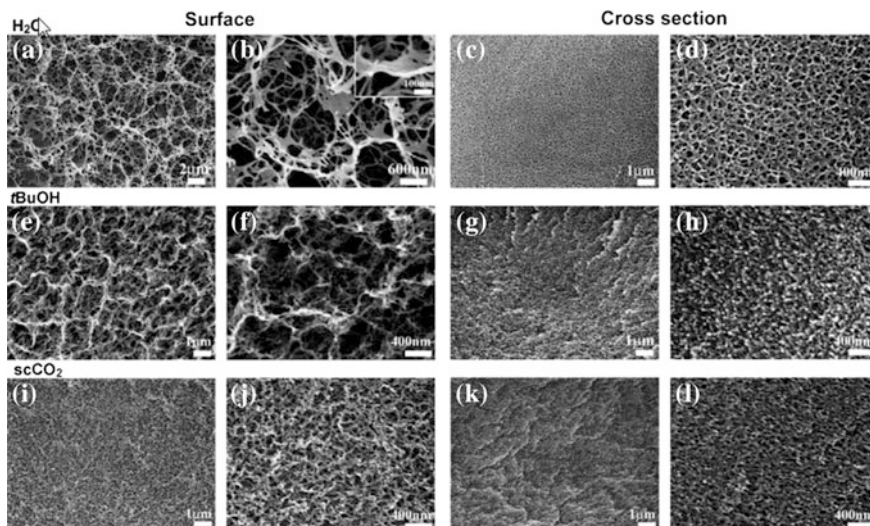


Fig. 15.5 SEM images of aerogels prepared from 4 wt% cellulose in aqueous LiOH/urea solution, regenerated with EtOH, and either freeze-dried from H₂O (a–d) or tBuOH (e–h) or dried from CO₂ (i–l) as indicated. (a), (e), (i) Low-magnification and (b), (f), (j) high-magnification images of the surface; (c), (g), (k) low-magnification and (d), (h), (l) high-magnification images of the cross sections of the aerogels. The inset in part (b) shows the SEM image of a tilted sample (Cai et al. 2008)

from the difference in regenerating condition; i.e., the surface was subjected to a drastic change in liquid composition, whereas the inside should have experienced gradual composition changes, leading to slow coagulation. XRD diagrams of the aerogels showed that the cellulose I structure was completely lost by dissolution–regeneration, and the pattern of aerogels was that of a poorly crystalline cellulose II. BET analysis of the aerogels gave surface area of around 200 m² g^{−1}. The mesopore analysis by Barret–Joyner–Harrenda (BJH) method gave wide mesopore size distributions, mostly in the range of 10–100 nm. The average mesopore diameter of aerogels was 13–20 nm determined by the BJH method.

Cellulose aerogels produced by NMMO/NBnMO method displayed porous structures with specific density and surface area ranged 0.05–0.26 g cm^{−3} and 172–284 m² g^{−1}, respectively, with increasing density at higher cellulose contents (Liebner et al. 2007, 2008). Among the tested regenerating solvents, ethanol gave the lowest specific densities upon supercritical drying at 40 °C and 100 bars and the highest retaining volume of about 70 %.

In the ionic liquid method, the morphology of the aerogels was changed with the number of FT treatment cycles (Li et al. 2011). With one FT treatment, the aerogel showed a porous structure. The distribution of the pores became denser with the increase in the FT treatment cycles. However, the microporous structure disappeared, and a dense film-like structure, which was associated with common open-pore web structure, was observed from the samples after quintuplicate FT

277 treatment. The film-like structure rather than a network structure was observed for
278 the samples after septuplicate and decuplicate FT treatment. The construction of
279 cellulose fibril networks was ascribed to the formation of the ionic liquid crystal
280 during the freezing process. Despite the influence of the wood/ionic liquid solution
281 concentration on the density of the network, the frequency of crystallization was
282 considered as the vital parameter to form the mesh structure.

283 Cellulose aerogels prepared via ultrasonication exhibited extremely low bulk
284 densities in the range of 1.3×10^{-3} – 17.0×10^{-3} g cm⁻³ (Chen et al. 2011) and
285 porosities of 98.94–99.91 %. They had a 3D open-porous fibrillar network structure
286 of continuous nanofibers (approximately 30–150 nm in width and several hundred
287 microns long), indicating that the CNFs self-assembled via hydrogen bonding
288 during the freeze-drying process, thus organizing them into long nanofibers and
289 formation a porous network structure. The distribution of the pores became denser
290 with the increase in the solid content of the hydrogels. Most of the microporous
291 structure disappeared when the CNF content was higher than 0.5 %, and a dense 2D
292 sheet-like structure, organized by small CNFs (around 20–30 nm wide and several
293 microns long) with only a few aggregates, was observed.

294 15.2.2.3 Thermal Properties

295 Thermogravimetric analysis showed the degradation temperature of cellulose
296 aerogels synthesized by the alkali/urea method was about 300–310 °C (Cai et al.
297 2012). The degradation point of the aerogels fabricated by the sonication method
298 was in the range of 325–337 °C. This degradation point was much higher than that
299 of original wood fibers (210 °C) (Chen et al. 2011). The cellulose aerogels showed
300 a very low thermal conductivity of $0.025 \text{ W m}^{-1} \text{ K}^{-1}$, which was slightly lower
301 than that [$0.0295 \text{ W m}^{-1} \text{ K}^{-1}$, (Sai et al. 2014)] of BC aerogels (Cai et al. 2012).

302 15.2.2.4 Mechanical Properties

303 In Cai et al.'s work (Cai et al. 2012), the tensile modulus and strength of cellulose
304 aerogels were determined as 72.0 and 12.4 MPa, respectively, which was much
305 higher than the compression modulus, 0.27 MPa (Sai et al. 2013), of BC aerogels.
306 Chen et al. found that their cellulose aerogels exhibited high flexibility and ductility
307 because of the high aspect ratio, high crystallinity, high CNF mechanical properties,
308 and an entangled 3D or 2D microstructure (Chen et al. 2011). As shown in
309 Fig. 15.6a–c, an aerogel with approximate dimensions of $5.44 \times 5.44 \times 0.59 \text{ cm}^3$
310 and a bulk density of 2.6×10^{-3} g cm⁻³ could be repeatedly bent without
311 destroying its structural integrity. The compression property of the aerogels was
312 also tested (Fig. 15.6d–f). A cylindrical aerogel with an approximate radius of
313 1.05 cm, a height of 1.67 cm, and density of 9.2×10^{-3} g cm⁻³ could be easily
314 compressed by hand into a sheet about 0.09 cm thick without disintegrating. The
315 obtained dense sheet with a bulk density of 0.17 g cm^{-3} could also be folded easily.

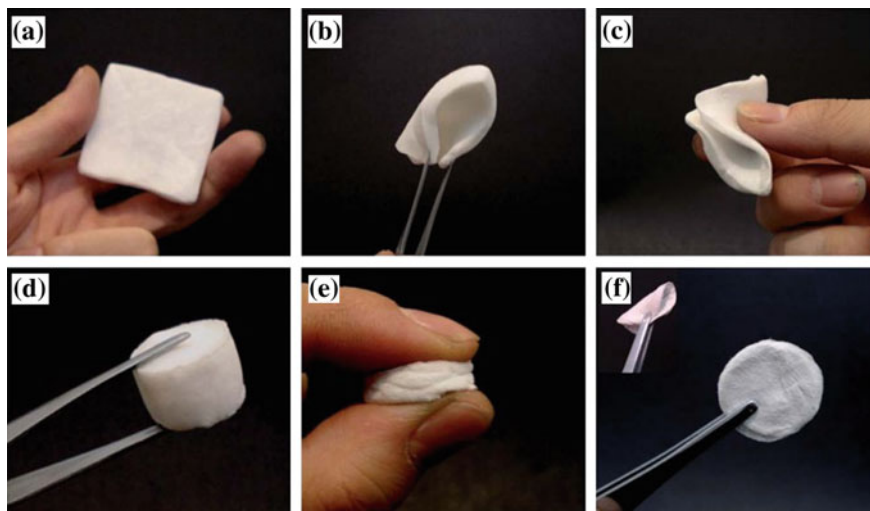


Fig. 15.6 A demonstration of the flexibility and deformability of the aerogels. **a–c** The aerogel with dimensions of about $5.44 \times 5.44 \times 0.59 \text{ cm}^3$ can be repeatedly bent as foldable as conventional paper. **d–f** Aerogel with a diameter of 2.10 cm and height of 1.67 cm can be compressed into a circuit sheet about 0.09 cm thick by hand; the obtained sheet can also be folded easily (Chen et al. 2011)

15.2.3 Cellulose Aerogels Prepared from Wastes

15.2.3.1 Fabrication Methods

In Nguyen et al.'s work (Nguyen et al. 2013, 2014), recycled cellulose fibers from paper waste were dispersed into a NaOH/urea solution by sonicating for 6 min. Thereafter, the solution was placed in refrigerator for more than 24 h to allow gelation of the solution. After the solution was frozen, it was then thawed at room temperature and then followed by immersing into ethanol (99 vol.%) for coagulation. After coagulation, solvent exchange was carried out by immersing the gel in DI water for 2 days. The sample was then frozen in a freezer at $-18 \text{ }^\circ\text{C}$ for 12 h. After that, freeze drying is carried out for 2 days with a freeze dryer to obtain the desired aerogel.

Feng et al. dispersed recycled cellulose fibers and Kymene cross-linker in 30 ml DI water by sonicating for 10 min (Feng et al. 2015). The suspension was then placed in a refrigerator at $-18 \text{ }^\circ\text{C}$ for more than 24 h to allow the gelation. The cellulose aerogel was obtained by freeze-drying the gel at $-98 \text{ }^\circ\text{C}$ for 2 days using a freeze dryer. Thereafter, the cellulose aerogel was further cured at $120 \text{ }^\circ\text{C}$ for another 3 h to cross-link completely the Kymene molecules.

In Jin's work (Jin et al. 2015), waste newspaper (WNP) pieces were dispersed into 1-allyl-3-methylimidazolium chloride (AMImCl) in a 20-mL beaker. The beaker



335 was immediately immersed in an oil bath at 80 °C under vigorous stirring for 4 h to
336 form a homogeneous mixture. Finally, a dark, amber-colored, viscous WNP sus-
337 pension was obtained. The resultant WNP solution was completely cast in Teflon
338 molds, took off air bubble in a vacuum oven, and then immediately coagulated in the
339 water to obtain a regenerated cellulose hydrogel. It was washed with excess
340 deionized water until the residual chemical reagents were absolutely removed. Then,
341 the prepared hydrogels were freeze-drying in a vacuum freeze dryer at -50 °C for
342 48 h.

343 Li et al. used waste wheat straw powder to synthesize cellulose aerogels (Li et al.
344 2014). Wheat straw was first treated by a mixed solution of benzene/absolute
345 ethanol (2:1 v/v) in a Soxhlet extractor at 90 °C for 6 h. Then, the treated sample
346 was air-dried and treated with a 10 % NaClO₂ solution at 75 °C for 5 h. The next
347 step was to collect the sample by filtration, wash it three times with DI water, and
348 then immediately treat it with 2 % NaOH at 90 °C for 2 h. The product was again
349 collected by filtration and washed three times with DI water before treating it with
350 1 % HCl at 80 °C for 2 h. Finally, the purified cellulose was collected by filtration,
351 washed three times the deionized water, and dried at 60 °C for 24 h. The purified
352 cellulose was added to a 10 % aqueous solution of NaOH/polyethylene glycol
353 (PEG) (9:1 wt/wt) with magnetic stirring for 5 h to form a homogeneous solution.
354 The solution was frozen for 12 h at -15 °C and then subsequently thawed at
355 ambient temperature with vigorous stirring for 30 min. This process was repeated at
356 least 3 times. The product was successively regenerated by 1 % HCl solution, DI
357 water, and tert-butanol until the formation of an amber-like hydrogel. Finally, the
358 resultant cellulose hydrogel samples were freeze-dried at -30 °C for 48 h.

359 15.2.3.2 Hydrophobic Coating Methods

360 As the cellulose aerogels developed in Sect. 2.3.1 were hydrophilic, the as-prepared
361 cellulose aerogels were coated with a hydrophobic coating agent on their highly
362 porous networks to form super-hydrophobic cellulose aerogels. Silane reagents
363 such as methyltrimethoxy silane (MTMS) and trimethylchlorosilane (TMCS) were
364 usually used as the coating agents via a CVD method (Feng et al. 2015; Jin et al.
365 2015; Li et al. 2014; Nguyen et al. 2013, 2014). The cellulose aerogel sample and
366 an open glass vial containing MTMS/TMCS were placed in a big container. The
367 container was then capped and heated at 70 °C for 3 or 12 h for the silanation
368 reaction. Thereafter, the coated sample was placed in a vacuum oven to remove the
369 excess coating reagent until the pressure reaches 0.03 mbar.

370 15.2.3.3 Environmental Stability

371 The MTMS-coated cellulose aerogels had super-hydrophobicity on both their
372 external and internal surfaces. Large water contact angles of 153.5° and 150.8°
373 were obtained, respectively, thus proving that the hydrophobic coating was

374 successfully covered the whole aerogel networks. The samples were then exposed
 375 in normal ambient atmosphere for five months. The water contact angles on the
 376 external surface and the cross section did not show any obvious change with time,
 377 confirming the excellent hydrophobicity stability of the MTMS-coated recycled
 378 cellulose aerogels (Feng et al. 2015).

379 15.2.3.4 Morphology Control

380 Figure 15.7 showed photographs and SEM images of the developed recycled cel-
 381 lulose aerogels (Feng et al. 2015; Nguyen et al. 2013; Nguyen et al. 2014). The
 382 recycled cellulose aerogels were formed via hydrogen bonding between the
 383 self-assembled cellulose fibers (Isobe et al. 2012). Besides, Kymene molecules
 384 could diffuse and react with the cellulose fiber surface to form the hydrogen
 385 bonding and also cross-linked with the surrounding Kymene molecules. The uti-
 386 lization of Kymene as a cross-linker combined the reinforcement and protection
 387 mechanisms (Nordell 2006) during the gelation process, which thus ensured the
 388 resultant aerogels with a robust structure and good flexibility. In contrast to the
 389 mesopores (2–50 nm) of the aerogels formed by the cellulose nanofibers, highly
 390 porous structures of the cellulose aerogels with macropores (>50 nm) could be
 391 clearly observed in SEM images of Fig. 15.7c–f. Their macropores were possibly
 392 caused by the larger size of the recycled cellulose fibers, obtained from the paper
 393 waste. Figure 15.7c, d shows the morphologies of the cellulose aerogels with
 394 cellulose concentrations of 0.25 and 1.00 wt%, respectively. The aerogel with the
 395 higher cellulose concentration (1.0 wt%) had a more compacted network and lower

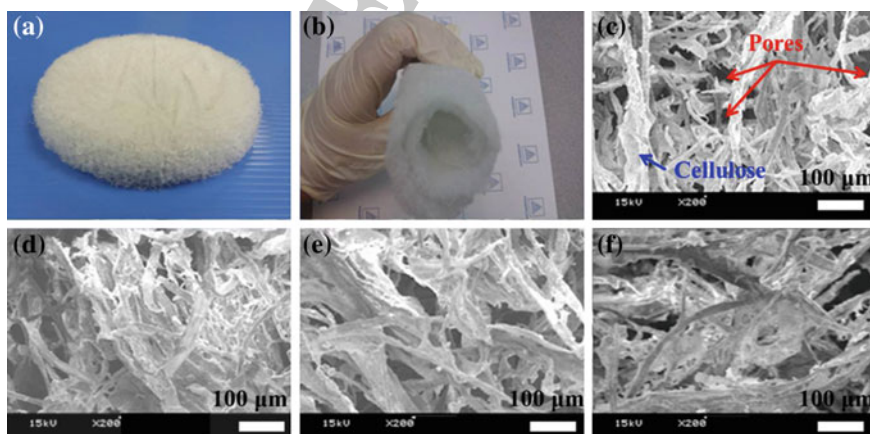


Fig. 15.7 **a** Super-hydrophobic recycled cellulose aerogel, **b** flexibility of the large-scale cellulose aerogel ($38 \times 38 \times 1$ cm) containing 0.60 wt% of the cellulose fibers, SEM images of the cellulose aerogels with different ratios of cellulose fibers (wt%) and kymene (μ l): **c** 0.25:5, **d** 1.00:5, **e** 0.60:5 and **f** 0.60:20 (Feng et al. 2015)

396 porosity. However, an increase of Kymene from 5 to 20 μl did not significantly
397 impact the aerogel structures as shown in Fig. 15.7e, f.

398 In Jin et al.'s study, the aerogels exhibited a highly open-porous structure
399 (porosity $\approx 96.8\%$) consisting of interconnected uniform cellulose fibers. The
400 densities of the aerogels without and with silane modification were 0.020 and
401 0.029 g cm^{-3} , respectively (Jin et al. 2015). Li et al. found that the bulk densities of
402 the samples increased with the enhanced cellulose concentrations (Li et al. 2014).
403 The samples were referred as C1, C2, C4, and C8 with mass ratios of 1/100, 2/100,
404 4/100, and 8/100 cellulose to the NaOH/PEG solution. The bulk densities of C1, C2,
405 C3, and C4 were 44.9, 56.7, 80.7, and 148.0 mg cm^{-3} , respectively. The pore
406 configurations of C1 and C2 were dense, anfractuous, and multilayered, while the
407 pore distributions of C3 and C4 were relatively uniform. Some larger sheet and
408 blocky regions surrounding with pore structures were observed. This might be
409 attributed to the existence of undissolved fractional cellulose at high concentrations.
410 It was concluded that the concentration had a significant influence on the pore
411 structures of the aerogels. Specific surface areas and mean pore diameters of the
412 samples were in the ranges of 36.5–101 $\text{m}^2 \text{g}^{-1}$ and 16.2–18.3 nm, respectively.

413 15.2.3.5 Thermal Properties

414 Thermal conductivity of the recycled cellulose aerogel was 0.032 $\text{W m}^{-1} \text{K}^{-1}$
415 (Nguyen et al. 2014), which was comparable to those of good insulation materials
416 such as silica aerogel (0.026 $\text{W m}^{-1} \text{K}^{-1}$), wool (0.03–0.04 $\text{W m}^{-1} \text{K}^{-1}$), and Aspen
417 Aerogels products (0.021 $\text{W m}^{-1} \text{K}^{-1}$) (Sequeira et al. 2009; Nguyen et al. 2014).
418 A TGA test was performed for the sample in air. There was a weight loss of 23 % in
419 the temperature range of 25–230 $^{\circ}\text{C}$ due to the removal of absorbed water and some
420 urea trace left in the sample. Then, a weight loss of 42 % occurred in the range of
421 230–330 $^{\circ}\text{C}$ due to the degradation and burning of the cellulose aerogel structure.
422 There was small drop of the sample weight at 550–630 $^{\circ}\text{C}$ due to the oxidation of
423 some stable local structures of the aerogel.

424 15.2.3.6 Mechanical Properties

425 As shown in Fig. 15.7b, the large-scale cellulose aerogel was easily bent or rolled
426 without damaging its shape. The flexibility of the recycled cellulose aerogel was
427 comparable to that of nanocellulose aerogels (Chen et al. 2011). A qualitative test
428 was performed for the sample to investigate its mechanical strength by loading a
429 200 g weight on the sample for 1 h, 5 h, 1 day, and 5 days. No shape change of the
430 aerogel was found after the test durations. Tensile and compression tests were
431 performed for the aerogel samples. The yield and tensile strengths of the aerogel
432 were 1080 and 1470 N/m^2 , respectively, with a Young's modulus of 11 kPa
433 (Nguyen et al. 2014).

15.3 Conclusions and Future Perspectives

High energy consumption, climate changes, and the exhaust of fossil fuels require more sustainable and energy efficient construction solutions. In order to meet the demand of improved energy efficiency, the thermal insulation of building has an important role. As a result, it is essential to develop new insulation materials with low thermal conductivity for construction applications. Cellulose is a green, non-toxic, cheap, and abundant material. The combination of cellulose and aerogel structure has formed a novel and effective material for heat insulation. The extremely low thermal conductivity of $0.025\text{--}0.032\text{ W m}^{-1}\text{ K}^{-1}$ and good flexibility of cellulose aerogels make them a promising material for building heat insulation. The thermal stability limitation of cellulose aerogels can be overcome by combining with fire retardants or other heat insulation materials such as flexible silica aerogels.

References

- Al-Homoud DMS (2005) Performance characteristics and practical applications of common building thermal insulation materials. *Build Environ* 40(3):353–366. doi:[10.1016/j.buildenv.2004.05.013](https://doi.org/10.1016/j.buildenv.2004.05.013)
- Baetens R, Jelle BP, Gustavsen A (2011) Aerogel insulation for building applications: a state-of-the-art review. *Energy Build* 43(4):761–769. doi:[10.1016/j.enbuild.2010.12.012](https://doi.org/10.1016/j.enbuild.2010.12.012)
- Bheekhun N, Abu Talib AR, Hassan MR (2013) Aerogels in aerospace: an overview. *Adv Mater Sci Eng* 2013:18. doi:[10.1155/2013/406065](https://doi.org/10.1155/2013/406065)
- Briga-Sá A, Nascimento D, Teixeira N, Pinto J, Caldeira F, Varum H, Paiva A (2013) Textile waste as an alternative thermal insulation building material solution. *Constr Build Mater* 38:155–160. doi:[10.1016/j.conbuildmat.2012.08.037](https://doi.org/10.1016/j.conbuildmat.2012.08.037)
- Bryning MB, Milkie DE, Islam MF, Hough LA, Kikkawa JM, Yodh AG (2007) Carbon nanotube aerogels. *Adv Mater* 19(5):661–664. doi:[10.1002/adma.200601748](https://doi.org/10.1002/adma.200601748)
- Cai J, Kimura S, Wada M, Kuga S, Zhang L (2008) Cellulose aerogels from aqueous alkali hydroxide-urea solution. *ChemSusChem* 1(1–2):149–154
- Cai J, Liu S, Feng J, Kimura S, Wada M, Kuga S, Zhang L (2012) Cellulose-silica nanocomposite aerogels by in situ formation of silica in cellulose gel. *Angew Chem Int Ed Engl* 51(9):2076–2079. doi:[10.1002/anie.201105730](https://doi.org/10.1002/anie.201105730)
- Cannon RE, Anderson SM (1991) Biogenesis of bacterial cellulose. *Crit Rev Microbiol* 17(6):435–447. doi:[10.3109/10408419109115207](https://doi.org/10.3109/10408419109115207)
- Cervin NT, Aulin C, Larsson PT, Wågberg L (2012) Ultra porous nanocellulose aerogels as separation medium for mixtures of oil/water liquids. *Cellulose* 19(2):401–410
- Chang C, Zhang L (2011) Cellulose-based hydrogels: present status and application prospects. *Carbohydr Polym* 84(1):40–53
- Chen W, Yu H, Li Q, Liu Y, Li J (2011) Ultralight and highly flexible aerogels with long cellulose I nanofibers. *Soft Matter* 7(21):10360–10368
- Eichhorn SJ, Dufresne A, Aranguren M, Marcovich NE, Capadona JR, Rowan SJ, Weder C, Thielemans W, Roman M, Renneckar S, Gindl W, Veigel S, Keckes J, Yano H, Abe K, Nogi M, Nakagaito AN, Mangalam A, Simonsen J, Benight AS, Bismarck A, Berglund LA, Peijs T (2010) Review: current international research into cellulose nanofibres and nanocomposites. *J Mater Sci* 45(1):1–33

- 477 Fan Z, Marconnet A, Nguyen ST, Lim CYH, Duong HM (2014) Effects of heat treatment on the
478 thermal properties of highly nanoporous graphene aerogels using the infrared microscopy
479 technique. *Int J Heat Mass Transf* 76:122–127. doi:[10.1016/j.ijheatmasstransfer.2014.04.023](https://doi.org/10.1016/j.ijheatmasstransfer.2014.04.023)
- 480 Feng J, Nguyen ST, Fan Z, Duong HM (2015) Advanced fabrication and oil absorption properties
481 of super-hydrophobic recycled cellulose aerogels. *Chem Eng J* 270:168–175. doi:[10.1016/j.cej.
2015.02.034](https://doi.org/10.1016/j.cej.2015.02.034)
- 482
- 483 Gesser HD, Goswami PC (1989) Aerogels and related porous materials. *Chem Rev* 89(4):765–
484 788. doi:[10.1021/cr00094a003](https://doi.org/10.1021/cr00094a003)
- 485 Hestrin S, Schramm M (1954) Synthesis of cellulose by *Acetobacter xylinum*. 2. Preparation of
486 freeze-dried cells capable of polymerizing glucose to cellulose. *Biochem J* 58(2):345–352
- 487 Innerlohinger J, Weber HK, Kraft G (2006) Aerocellulose: aerogels and aerogel-like materials
488 made from cellulose. *Macromol Symp* 244(1):126–135. doi:[10.1002/masy.200651212](https://doi.org/10.1002/masy.200651212)
- 489 Isobe N, Kimura S, Wada M, Kuga S (2012) Mechanism of cellulose gelation from aqueous
490 alkali-urea solution. *Carbohydr Polym* 89(4):1298–1300. doi:[10.1016/j.carbpol.2012.03.023](https://doi.org/10.1016/j.carbpol.2012.03.023)
- 491 Jelle BP (2011) Traditional, state-of-the-art and future thermal building insulation materials and
492 solutions—properties, requirements and possibilities. *Energy Build* 43(10):2549–2563. doi:[10.
1016/j.enbuild.2011.05.015](https://doi.org/10.1016/j.enbuild.2011.05.015)
- 493
- 494 Jin C, Han S, Li J, Sun Q (2015) Fabrication of cellulose-based aerogels from waste newspaper
495 without any pretreatment and their use for absorbents. *Carbohydr Polym* 123:150–156. doi:[10.
1016/j.carbpol.2015.01.056](https://doi.org/10.1016/j.carbpol.2015.01.056)
- 496
- 497 Kalia S, Dufresne A, Cherian BM, Kaith BS, Avérous L, Njuguna J, Nassiopoulos E (2011)
498 Cellulose-based bio—and nanocomposites: a review. *Int J Polym Sci*. doi:[10.1155/2011/
837875](https://doi.org/10.1155/2011/837875)
- 499
- 500 Keshk SM (2014) Bacterial cellulose production and its industrial applications. *J Bioprocess*
501 *Biotech* 04(02). doi:[10.4172/2155-9821.1000150](https://doi.org/10.4172/2155-9821.1000150)
- 502 Klemm D, Kramer F, Moritz S, Lindström T, Ankerfors M, Gray D, Dorris A (2011)
503 Nanocelluloses: a new family of nature-based materials. *Angew Chem Int Ed* 50(24):5438–5466
- 504 Li J, Lu Y, Yang D, Sun Q, Liu Y, Zhao H (2011) Lignocellulose aerogel from wood-ionic liquid
505 solution (1-allyl-3- methylimidazolium chloride) under freezing and thawing conditions.
506 *Biomacromolecules* 12(5):1860–1867
- 507 Li J, Wan C, Lu Y, Sun Q (2014) Fabrication of cellulose aerogel from wheat straw with strong
508 absorptive capacity. *Front Agric Sci Eng* 1(1):46. doi:[10.15302/j-fase-2014004](https://doi.org/10.15302/j-fase-2014004)
- 509 Liang H-W, Wu Z-Y, Chen L-F, Li C, Yu S-H (2015) Bacterial cellulose derived nitrogen-doped
510 carbon nanofiber aerogel: an efficient metal-free oxygen reduction electrocatalyst for zinc-air
511 battery. *Nano Energy* 11:366–376. doi:[10.1016/j.nanoen.2014.11.008](https://doi.org/10.1016/j.nanoen.2014.11.008)
- 512 Liebner F, Potthast A, Rosenau T, Haimer E, Wendland M (2007) Ultralight-weight cellulose
513 aerogels from NBnMO-stabilized lyocell dopes. *Res Lett Mater Sci* 2007:1–4. doi:[10.1155/
2007/73724](https://doi.org/10.1155/2007/73724)
- 514
- 515 Liebner F, Potthast A, Rosenau T, Haimer E, Wendland M (2008) Cellulose aerogels: highly
516 porous, ultra-lightweight materials. *Holzforschung* 62(2):129–135
- 517 Liebner F, Haimer E, Wendland M, Neouze MA, Schlutter K, Miethe P, Heinze T, Potthast A,
518 Rosenau T (2010) Aerogels from unaltered bacterial cellulose: Application of scCO₂ drying for
519 the preparation of shaped, ultra-lightweight cellulosic aerogels. *Macromol Biosci* 10(4):349–352
- 520 Mieck KP, Nechwatal A, Knobelsdorf C (1994) Potential applications of natural fibres in
521 composite materials. *Melliand Textilberichte* 75(11):892–898 + E228
- 522 Moon RJ, Martini A, Nairn J, Simonsen J, Youngblood J (2011) Cellulose nanomaterials review:
523 Structure, properties and nanocomposites. *Chem Soc Rev* 40(7):3941–3994
- 524 Nguyen ST, Nguyen HT, Rinaldi A, Nguyen NPV, Fan Z, Duong HM (2012) Morphology control
525 and thermal stability of binderless-graphene aerogels from graphite for energy storage
526 applications. *Colloids Surf A* 414:352–358. doi:[10.1016/j.colsurfa.2012.08.048](https://doi.org/10.1016/j.colsurfa.2012.08.048)
- 527 Nguyen ST, Feng J, Le NT, Le ATT, Hoang N, Tan VBC, Duong HM (2013) Cellulose aerogel
528 from paper waste for crude oil spill cleaning. *Ind Eng Chem Res* 52(51):18386–18391. doi:[10.
1021/ie4032567](https://doi.org/10.1021/ie4032567)
- 529



- 530 Nguyen ST, Feng J, Ng SK, Wong JPW, Tan VBC, Duong HM (2014) Advanced thermal
531 insulation and absorption properties of recycled cellulose aerogels. *Colloids Surf A* 445:128–
532 134. doi:[10.1016/j.colsurfa.2014.01.015](https://doi.org/10.1016/j.colsurfa.2014.01.015)
- 533 Nordell P (2006) Wet strength development of paper. Lulea University of Technology
- 534 Oshima T, Sakamoto T, Ohe K, Baba Y (2014) Cellulose aerogel regenerated from ionic liquid
535 solution for immobilized metal affinity adsorption. *Carbohydr Polym* 103:62–69. doi:[10.1016/
536 j.carbpol.2013.12.021](https://doi.org/10.1016/j.carbpol.2013.12.021)
- 537 Pierre AC, Pajonk GM (2002) Chemistry of Aerogels and Their Applications. *Chem Rev* 102
538 (11):4243–4266. doi:[10.1021/cr0101306](https://doi.org/10.1021/cr0101306)
- 539 Pircher N, Veigel S, Aigner N, Nedelec JM, Rosenau T, Liebner F (2014) Reinforcement of
540 bacterial cellulose aerogels with biocompatible polymers. *Carbohydr Polym* 111:505–513.
541 doi:[10.1016/j.carbpol.2014.04.029](https://doi.org/10.1016/j.carbpol.2014.04.029)
- 542 Pour G, Beauger C, Rigacci A, Budtova T (2015) Xerocellulose: lightweight, porous and
543 hydrophobic cellulose prepared via ambient drying. *J Mater Sci* 50(13):4526–4535. doi:[10.
544 1007/s10853-015-9002-4](https://doi.org/10.1007/s10853-015-9002-4)
- 545 Sai H, Xing L, Xiang J, Cui L, Jiao J, Zhao C, Li Z, Li F (2013) Flexible aerogels based on an
546 interpenetrating network of bacterial cellulose and silica by a non-supercritical drying process.
547 *J Mater Chem A* 1(27):7963. doi:[10.1039/c3ta11198a](https://doi.org/10.1039/c3ta11198a)
- 548 Sai H, Xing L, Xiang J, Cui L, Jiao J, Zhao C, Li Z, Li F, Zhang T (2014) Flexible aerogels with
549 interpenetrating network structure of bacterial cellulose–silica composite from sodium silicate
550 precursor via freeze drying process. *RSC Adv* 4(57):30453. doi:[10.1039/c4ra02752c](https://doi.org/10.1039/c4ra02752c)
- 551 Sequeira S, Evtuguin DV, Portugal I (2009) Preparation and properties of cellulose/silica hybrid
552 composites. *Polym Compos* 30(9):1275–1282
- 553 Stamm AJ, Tarkow H (1950) Penetration of cellulose fibers. *J Phys Colloid Chemistry* 54(6):745–
554 753
- 555 Wang Z, Liu S, Matsumoto Y, Kuga S (2012) Cellulose gel and aerogel from LiCl/DMSO
556 solution. *Cellulose* 19(2):393–399. doi:[10.1007/s10570-012-9651-2](https://doi.org/10.1007/s10570-012-9651-2)
- 557 Wicklein B, Kocjan A, Salazar-Alvarez G, Carosio F, Camino G, Antonietti M, Bergstrom L
558 (2015) Thermally insulating and fire-retardant lightweight anisotropic foams based on
559 nanocellulose and graphene oxide. *Nat Nanotechnol* 10(3):277–283. doi:[10.1038/nnano.2014.
560 248](https://doi.org/10.1038/nnano.2014.248)
- 561 Yamanaka S, Watanabe K, Kitamura N, Iguchi M, Mitsuhashi S, Nishi Y, Uryu M (1989) The
562 structure and mechanical properties of sheets prepared from bacterial cellulose. *J Mater Sci* 24
563 (9):3141–3145. doi:[10.1007/BF01139032](https://doi.org/10.1007/BF01139032)
- 564 Zimmermann T, Pöhler E, Geiger T (2004) Cellulose fibrils for polymer reinforcement. *Adv Eng*
565 *Mater* 6(9):754–761. doi:[10.1002/adem.200400097](https://doi.org/10.1002/adem.200400097)

Author Query Form

Book ID : **334146_1_En**
 Chapter No.: **15**



Please ensure you fill out your response to the queries raised below and return this form along with your corrections

Dear Author

During the process of typesetting your chapter, the following queries have arisen. Please check your typeset proof carefully against the queries listed below and mark the necessary changes either directly on the proof/online grid or in the 'Author's response' area provided below

Query Refs.	Details Required	Author's Response
AQ1	Reference "Sai et al. (2015)" are cited in the text but not provided in the reference list. Please provide the respective reference in the list or delete that citation.	
AQ2	Please check the clarity of the phrase 'the inside observed on' in the sentence 'For the cellulose...of unique structure.'	

MARKED PROOF

Please correct and return this set

Please use the proof correction marks shown below for all alterations and corrections. If you wish to return your proof by fax you should ensure that all amendments are written clearly in dark ink and are made well within the page margins.

<i>Instruction to printer</i>	<i>Textual mark</i>	<i>Marginal mark</i>
Leave unchanged	... under matter to remain	Ⓟ
Insert in text the matter indicated in the margin	∧	New matter followed by ∧ or ∧ [Ⓢ]
Delete	/ through single character, rule or underline or ┌───┐ through all characters to be deleted	Ⓞ or Ⓞ [Ⓢ]
Substitute character or substitute part of one or more word(s)	/ through letter or ┌───┐ through characters	new character / or new characters /
Change to italics	— under matter to be changed	↙
Change to capitals	≡ under matter to be changed	≡
Change to small capitals	≡ under matter to be changed	≡
Change to bold type	~ under matter to be changed	~
Change to bold italic	≈ under matter to be changed	≈
Change to lower case	Encircle matter to be changed	≡
Change italic to upright type	(As above)	⊕
Change bold to non-bold type	(As above)	⊖
Insert 'superior' character	/ through character or ∧ where required	Υ or Υ under character e.g. Υ or Υ
Insert 'inferior' character	(As above)	∧ over character e.g. ∧
Insert full stop	(As above)	⊙
Insert comma	(As above)	,
Insert single quotation marks	(As above)	ʹ or ʸ and/or ʹ or ʸ
Insert double quotation marks	(As above)	“ or ” and/or ” or ”
Insert hyphen	(As above)	⊞
Start new paragraph	┌	┌
No new paragraph	┐	┐
Transpose	└┐	└┐
Close up	linking ○ characters	○
Insert or substitute space between characters or words	/ through character or ∧ where required	Υ
Reduce space between characters or words		↑